Surface Properties of Polyurethane Powder Lacquers Modified with Polysiloxane-Methacrylic Core-Shell Nanoparticles

Barbara Pilch-Pitera

Faculty of Chemistry, Department of Polymer Science, Rzeszów University of Technology, Al. Powstańców Warszawy 6, 35-959 Rzeszów, Poland

Received 14 January 2011; accepted 15 March 2011
DOI 10.1002/app.34506
Published online 8 August 2011 in Wiley Online Library (wileyonlinelibrary.com).

ABSTRACT: Non- and core-shell nanoparticles-containing polyurethane-based powder coating systems, cross-linked with allophanate bonds containing polyisocyanates were examined. The surface structure of the powder coatings were investigated with a confocal microscopy and polarized optical microscopy (POM) using reflected light. The three-dimensional surface topography and the values of surface roughness were determined. The surface structure was correlated with the chemical structure of the coatings and macroscopic surface behavior: surface free energy and gloss. These experimental results led to a better understanding of the development of surface topography and morphology and provide valuable information for the development of new polyurethane powder coating systems.
 J Appl Polym Sci 123: 807–814, 2012

Key words: polyurethanes; coatings; surfaces; microstructure; core-shell nanoparticles

INTRODUCTION

Nanotechnology applications in coatings have shown remarkable growth in recent years.[1–6] This is a result of the following factors: increased availability of nano-scale materials, advancements in processes that can control coating structure at the nanoscale as well as possibility of new more advantageous properties of coating materials. Incorporation of nano-scale organic or inorganic materials to organic coatings has become of the most prevalent approaches leading to nanocomposite coating products. The nanocomposite made out of two different materials would have very high interfacial contact. The compatibility of nanomaterials with polymeric materials is expected to be markedly enhanced due to the possibility of modifying the chemical or physical interactions at polymer–filler interface. The small size of nanoparticles offers two features: high surface area contact with a host polymer and optical clarity of the nanocomposite. Both of which are important in clear coating applications. Unless the refractive index can be matched to that of the coating resin, adding nanopaticles cause light scattering that leads to reduction or elimination of film clarity. Since nanoparticles are much smaller in size compared to the wavelength range of visible light (400–800 nm), they scatter very little light. Therefore, they can be added to a clear coating formulation with little or no adverse impact on visual characteristics. The increased interfacial contact can cause significant shifts in properties of the overall composite compared to the properties of the organic phase alone.

In this article, the polyurethane powder coatings were modified by means of acrylic-polysiloxane nanopartiles. The unique structure of polysiloxane chain which constitutes the core of nanoparticle determined unique macroproperties of modified coatings. Because of high energy of Si—O—Si bond (550 kJ mol^{-1} vs. 340 kJ mol^{-1} for C—C or C—O) cleavage of polysiloxane chain is difficult. In consequence polysiloxanes have high temperature and chemical resistance. Additionally, they have high elasticity, specifically at low temperatures (very low T_g) because of high chain mobility (about 145° angle of Si—O—Si linkage). Polysiloxanes show excellent gas permeability, because of loose packing of chains. Moreover high hydrophobicity of CH_3— groups and their migration to coating surface cause achieving very low surface free energy (SFE).

The glass temperature of core of nanoparticles with core-shell structure should be lower than the glass temperature of the shell.[7–9] The shell protects the core from liquidation during extrusion and guaranties well distribution of nanoparticles in the lacquer. Melting of the shell and release of core contents takes place during hardening of the coating. Generally, core-shell nanoparticles can be

Correspondence to: B. Pilch-Pitera (barbpi@prz.edu.pl).
Contract grant sponsor: Polish Ministry of Science and Higher Education; contract grant number: N N507 503338.

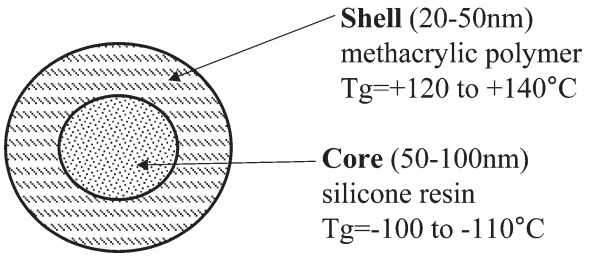

Figure 1 The structure of polysiloxane-methacrylic core-shell nanoparticle.

incorporated into polymer matrix by mechanically melt blending as nano-filler particles.

The objectives of this article were results to study to determine the effects of nanoparticles on the surface properties of polyurethane powder coatings. Confocal and polarized optical microscopy (POM) was employed in visualization of the surface morphology and the supermolecular structures of obtained coatings. The measurements of the ATR FT-IR, DSC, contact angle with various liquids (diiodomethane, formamide, and water), the surface roughness, and gloss (for the angles of 20°, 60°, and 85°) were used to characterize the powder coatings and correlating their structure with the macroscopic surface behavior (wettability, roughness, and gloss characteristics).

The relationship between surface properties and the nanopowder content was discussed.

EXPERIMENTAL

Raw materials and reagents

Isophorone diisocyanate (IPDI)—Desmodur I and 4,4′-dicyclohexylmethane diisocyanate (H_{12}MDI)—Desmodur W were obtained from Bayer A.G. (Leverkusen, Germany). Ethanol (ET), 2-propanol (PR), 1-butanol (BU), and 1-hexanol (HE) from Aldrich (Buchs, Switzerland). The 3,5-dimethylpirazole (DMP) from Aldrich (Buchs, Switzerland). Rucote 102—polyester resin based on isophthalic acid and neopentyl glycol, acid value: 11–14 mg KOH g^{-1}, hydroxyl value: 35–45 mg KOH g^{-1}, T_g: 59°C (RU102), from Bayer A.G. (Leverkusen, Germany). WorleeAdd 902, WorléeAdd ST-70, and Resiflow PH 240 from Worlée—Chemie G.m.b.H (Lauenburg, Germany). Core-shell nanoparticles (Fig. 1) were synthesized by Kozakiewicz et al.[9]

Synthesis of curing agents for powder lacquers

Synthesis of allophanate bonds containing polyisocyanates

Allophanate bonds containing polyisocyanates were used as curing agents. Polyisocyanates were synthesized according to the procedure as described in details in my earlier reports.[10,11] The synthesis covered three stages: synthesis of urethane polyisocyanate, synthesis of allophanate, and blocking reaction. The obtained products were marked with symbols, e.g., IPDI/BU, where individual segments stand for the names of the feeds used. The molecular structure of internally-blocked polyisocyanates contained allophanate bonds was presented in Figure 2.

Preparing lacquer compositions and coatings

Two types of the lacquer compositions were prepared: unmodified and modified with core-shell nanoparticles. Unmodified lacquer compositions consist of: blocked polyisocyanates, polyester resin RUCOTE 102 (the NCO : OH molar ratio = 1 : 1), WorléeAdd 902 (1.5%), WorléeAdd ST-70 (0.5%), and Resiflow PH-240 (3%). The modified compositions with core-shell nanoparticles were prepared by addition of the nanopowder to unmodified composition in amounts 1, 3, and 5%.

The mixture was break-up, melted, cooled, and pulverized to the average particle size of 60 μm. The final powder coating was applied manually to steel panels and cured at 150–160°C for 30–50 min. The obtained compositions were marked with symbols, e.g., IPDI/E/5%N, where individual segments stand for the names of the feeds used.

Measurements

ATR FT-IR spectroscopy

Attenuated total reflection (ATR) spectra were recorded by reflection technique with a Nicolet 6700

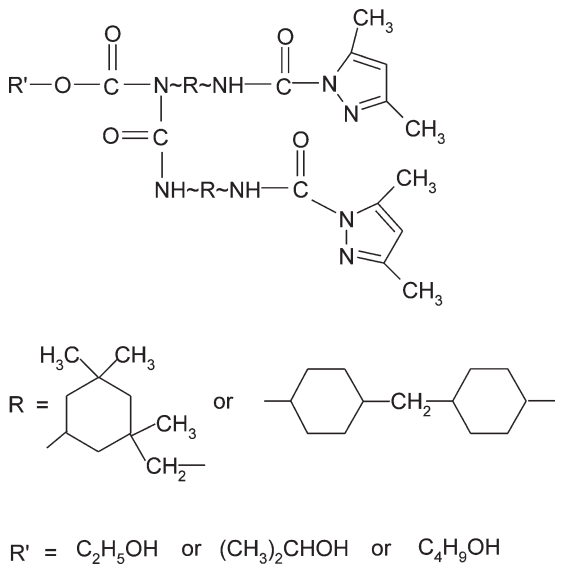

Figure 2 The molecular structure of the internally blocked polyisocyanate-contained allophanate bonds.

TABLE I
Specifications of the Coatings Water Contact Angle and Roughness

Symbol of coating		H_{12}MDI/E	H_{12}MDI/E/1%N	H_{12}MDI/E/3%N
Water contact angle	Θ (deg)	85.17	92.65	95.33
Roughness parameters	R_a (μm)	0.394	0.483	0.492
	R_z (μm)	2.209	3.088	3.278
	R_t (μm)	2.612	3.757	3.902
	R_q (μm)	0.504	0.624	0.624
	R_{max} (μm)	2.612	3.757	3.902
	R_{ms} S. (deg)	0.059	0.080	0.093
	Sep (μm)	0.5	0.5	0.5
	*R*pc (peak cm^{-1})	37.573	56.360	56.360

FTIR instrument from Thermo Scientific equipped with a diamond crystal. The ATR experiment consists of placing the sample to be analyzed in contact with a high refractive index material (diamond, $n = 2.3$) through which the infrared beam is confirmed.

Polarized optical microscopy (POM)

The surface of the powder lacquers were observed with the use of a Nikon ECLIPSE LV100 POL polarizing light optical microscope equipped with a polarizing filters, THMS-600 Linkam microscope hot-stage, and a Linkam TMS-94 temperature controller with liquid nitrogen cooling, used to provide the thermal control of the samples under the microscope within the temperature range from 25 to 180°C. Images were recorded on DS5Mc-L1 camera linked to computer via NIS—Elements Basic Research software.

Surface topography measurements

The surface topography of the powder lacquers were investigated with the use of a NanoFocus Confocal Microscope (CM) μsurf explorer with capability of an accurate three-dimensional measurement and submicron imaging, with outstanding 2-nm resolution. The 505-nm diode combined with optics specifically enables resolution in *z*-direction 2–20 nm as well as in *x*, *y*-direction 500–3100 nm.

The values of R_a, R_z, R_t, R_q, R_{max}, R_{ms} S, and R_{pc} were used to characterize the coating roughness parameters. These symbols mean as follow:

- R_a—arithmetic mean deviation of the assessed profile,
- R_z—max. height of the profile within a sampling length,
- R_t—total height of the profile on the evaluation length,
- R_q—root mean square deviation of the assessed profile,
- R_{max}—max. profile peak height within a sampling length,
- R_{ms} S—root-mean-square slope of the profile within a sampling length. The result is expressed in degrees,
- R_{pc}—peak count, number of peaks per centrimetres. Each peak being higher that the upper threshold, and falling under the lower threshold. The threshold is defined by a band, symmetrically separated (Sep) around the mean line (if Sep = 0.5 μm, than the size of side of the mean is ±0.25 μm). The result is expressed in peaks cm^{-1}.

The values specific for the coatings roughness were collected in Table I.

Surface roughness measurements

The surface roughness of the powder lacquers were investigated by means of profile method with the use a Mahr GmbH Göttingen apparatus, Mar Surf PS1 according to PN-EN ISO[12] standard.

Measurements were made at temperature 21°C ± 0.1°C, $L_T = 5600$ mm and $L_C = 0.800 \times 5^N$. The values of R_z and R_a were used to characterize the coating roughness parameters.

Gloss

A micro-TRI-gloss tester from Byk Gardner was employed, according to the standard PN-EN ISO[13] for the angles of 20°, 60°, and 85°.

Differential scanning calorimetry (DSC)

A Mettler Toledo type 822^e differential calorimeter (DSC) with the Star^e System software was employed to analyze thermal properties of powder lacquers. The instrument was calibrated with the use of Zn and In standards. The samples (0.0010 g) were placed in aluminum crucibles. These were weighed to the nearest 0.00001 g and placed in the measuring chamber. The measurements were taken in the heating–cooling–heating cycle within the temperature range of 25–250°C, in the environment of nitrogen

which was passed at the rate of 30 cm^3 min^{-1}. The progressive heating was initiated at the rate of 10° min^{-1}.

Determination of surface free energy (SFE)

Surface free energy (γ_S), is quantified using a contact angle goniometer made by Cobrabid-Optic. As immersed liquids diiodomethane, formamide, and water were chosen. Measurements were realized at 22°C ± 1°C.

Contact angles of those three liquids with known values of γ_L, γ_L^{LW}, γ_L^+, and γ_L^- are put into the following equation (acid-base model by van Oss)[14]:

$$(\gamma_S^{LW}\gamma_{Li}^{LW})^{0,5}+(\gamma_S^+\gamma_{Li}^-)^{0,5}+(\gamma_S^-\gamma_{Li}^+)^{0,5}=\gamma_{Li}(1+\cos\Theta_i)/2$$

where γ refers to surface free energy, the subscripts Li and *S* refer to liquid and solid, and the superscripts LW, +, and − refers to dispersive, acid, and base components. The total surface free energy of the solid is then given by:

$$\gamma_S=\gamma_S^{LW}+\gamma_S^{AB}=\gamma_S^{LW}+2(\gamma_S^+\gamma_S^-)^{0,5}$$

Calculations based on these measurements produce a parameter (critical surface tension or surface free energy), which quantifies the characteristics of the solid and mediates the properties of the solid substrate.

RESULTS AND DISCUSSION

Blocked polyisocyanates were used as curing agents for investigated powder lacquer coatings. Those poly-isocyanates were synthesized from cycloaliphatic diisocyanates IPDI and H_{12}MDI, and from monohydric alcohols: methanol, ethanol, 2-propanol, 1-butanol, and 1-hexanol. On the basis of —NCO group content, ^{1}H NMR and ^{13}C NMR spectra and gel permeation chromatography analysis, the chemical structure of obtained products was confirmed. The commercial polyester resin Rucote 102 from Bayer made the principal component of the lacquer. The lacquer blends were prepared with the use of additives which improved leveling (Resiflow PH-240) and eliminated gas bubbles (WorleeAdd 902) in the hardening operation. The WorleeAdd ST-70 was used as a catalyst. To modify the surface properties, polysiloxane-methacrylic core-shell nanoparticles were introduced (in amount 1, 3, and 5%) at the lacquer blending stage. Unmodified samples and those modified with nanoparticles were used in studies on the hydrophobic effect as well as appearance and performance properties.

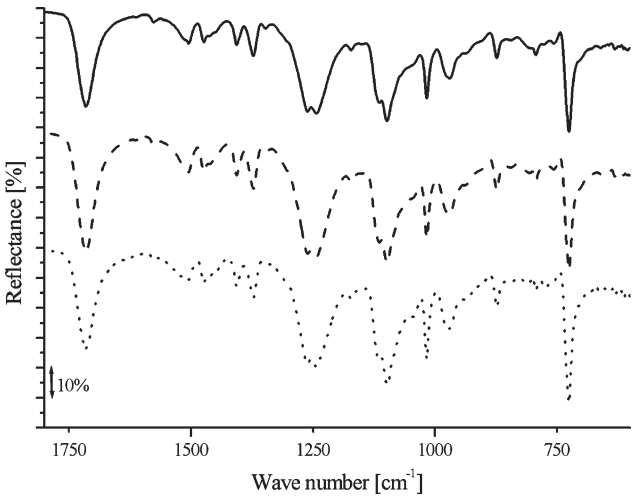

Figure 3 The ATR FT-IR spectra of the powder coating H_{12}MDI/E/1%N, H_{12}MDI/E/3%N, and H_{12}MDI/E/5%N.

ATR FT-IR spectroscopy

Reflection infrared spectra of H_{12}MDI/E/1%N, H_{12}MDI/E/3%N, and H_{12}MDI/E/5%N coatings were reported for comparison in Figure 3. The broad bands at 3360 cm^{-1} were assigned to NH stretching vibration of urethane, urea, and allophanate groups (invisible in Fig. 3). The C=O stretching vibration of urethane, urea, allophanate, and ester groups were responsible for the bands observed at 1715cm^{-1}. Weak broad bands at 1580 and 1610 cm^{-1} were connected to C—C ring stretching vibration of polyester resin which includes isophtalic acid. The band at 1372 cm^{-1} can be assigned to the so-called "umbrella" deformation of methyl groups from neopenthyl glycol and ethyl alcohol. The *N*—H scissors deformation vibration and C—N stretching vibration (amide II band) were split at 1536 cm^{-1}. In the spectra the bands from silicone resin were visible. The symmetric Si—CH_3 deformation vibration was observed as two bands at 1244 and 1260 cm^{-1}. The antisymmetrical Si—O—Si stretching vibrations generated the bands at 1170 and 1120 cm^{-1}. The band at 1050 cm^{-1} may be associated with the Si—C stretching and CH_3 rocking vibrations. The band that occurs at 793 cm^{-1} was due to the Si—C stretching vibration and CH_3 deformation vibration. In addition to the bands associated with the siloxane resin structure (1170 and 1120 cm^{-1} Si—O—Si stretching; 1050 cm^{-1} Si—C stretching and CH_3 rocking; 1244 cm^{-1} Si—CH_3 deformation), in this region also reflectance of polyester resin and polyisocyanate were occurred (1070cm^{-1} C—O—C stretching; 1230 cm^{-1} antisymmetrical C=O and O—CH_2 stretching and 1245 cm^{-1} C—N stretching (amide III band)). These bands may obscure bands associated with the silicone resin. The out-of-plane (rocking) weak band of

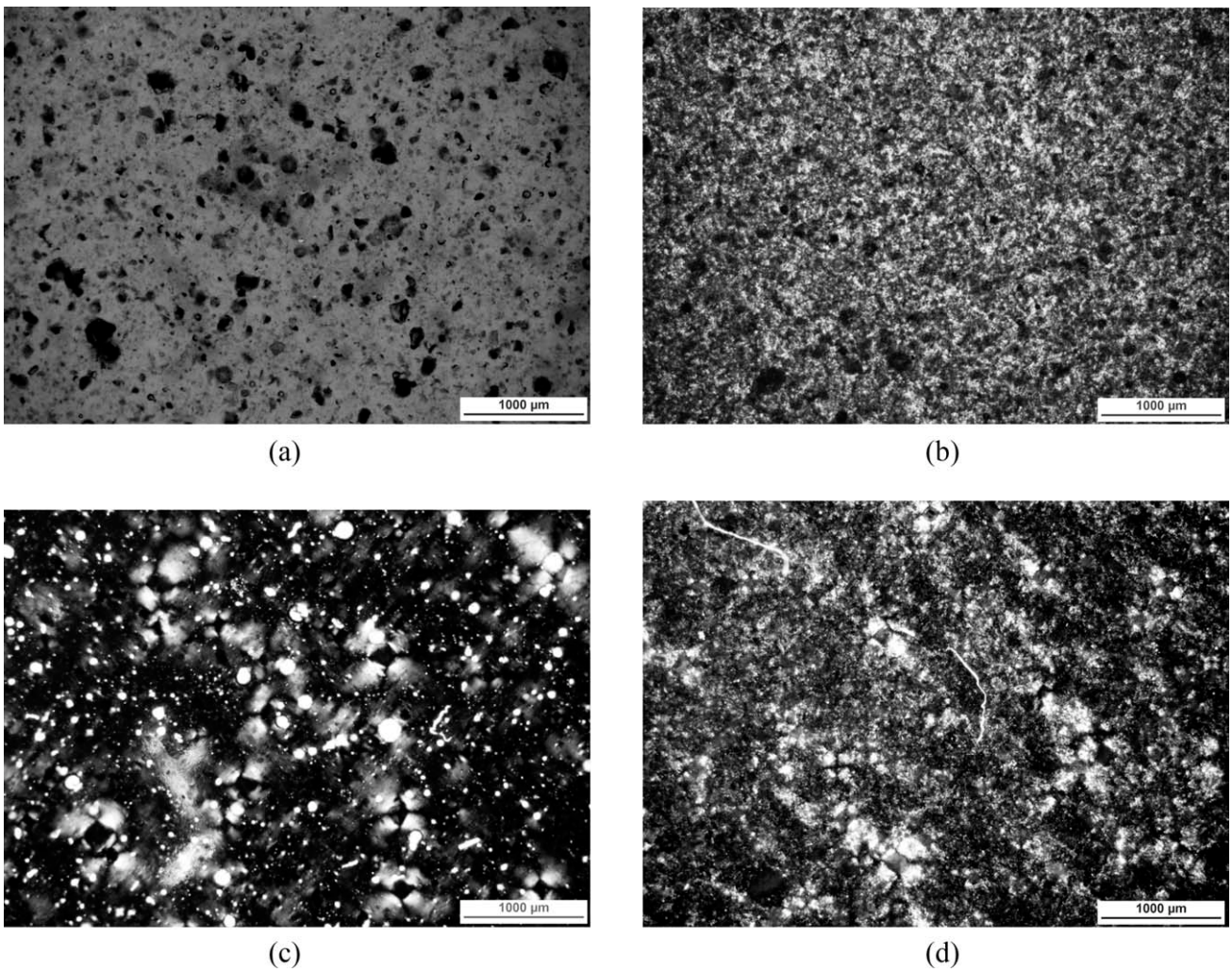

Figure 4 (a,b) The optical images of the powder coating H_{12}MDI/E (a) and H_{12}MDI/E/5%N (b). (c,d). The optical images of the powder coating H_{12}MDI/E (c) and H_{12}MDI/E/5%N (d) observed in the polarized light.

—CH_2— linear structure from alcohol, HDI, and resin was visible at 728 cm^{-1}.

Visualization of the coating surface with the use of a polarized optical microscope

The optical microscopic examination revealed that the surfaces of modified lacquers were less homogeneous than those of unmodified lacquers [Fig. 4(a,b)].

In the case of unmodified coatings, numerous crystalline structures could be observed in the polarized light [Fig. 4(c,d)]. For modified coats, a lower tendency to crystallize was noticed, as well as the declining number of crystallites for the increasing share of nano-powder in the samples.

The hard phase which were formed in the cross-linking process, composed of urethane bonds, ester bonds, and aromatic rings (derived from isophthalic acid), undergo micro-separation from flexible segments. The higher the micro-separation degree, the higher is the ability to crystallize.[15] Hydrogen bonds are formed between urethane groups and ester groups which are components of said hard phase; and that provides additional and favorable conditions for crystallization. The presence of the polymer nanoparticles incorporated in the PU structure pushes the polyurethane chains aside that reduces the tendency to micro-separation and create hydrogen bonds which makes a considerable impediment for the crystallization process.

Presentation of three-dimensional surface topography by confocal microscopy

Using this technique, the three-dimensional surface topographies of the powder coatings were obtained. This method is well-suited to the investigation of surface structures. The three-dimensional topographies of powder coatings were shown in Figure 5(a–c). The surface was smooth, the surfaces of the nanoparticles contained powder coatings that exhibit much larger irregularity and roughness (Fig. 6).

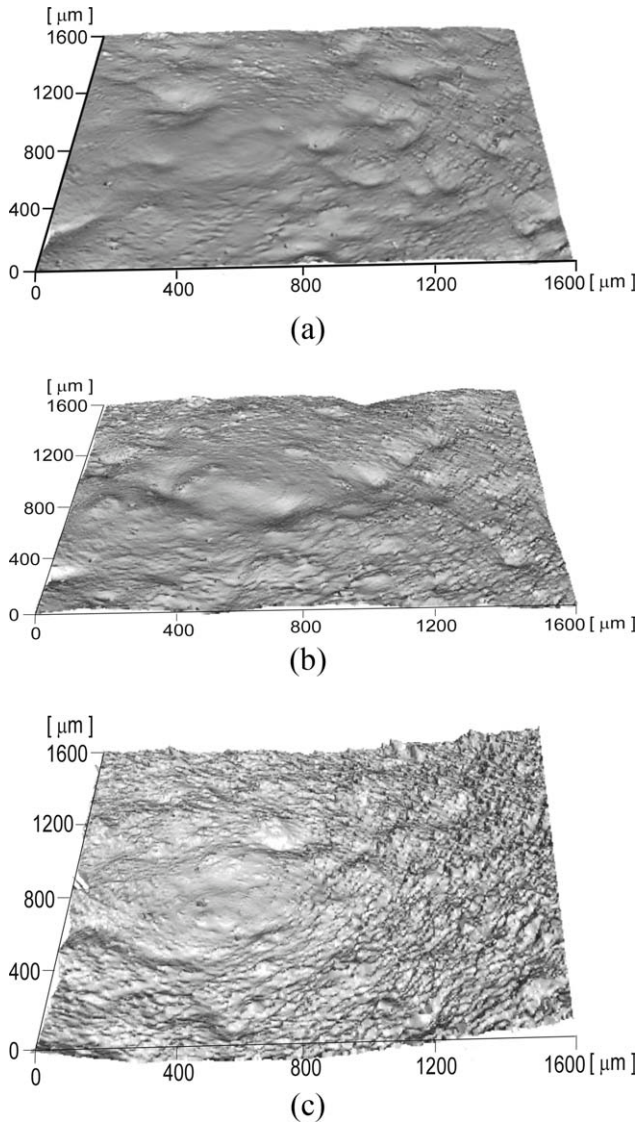

Figure 5 (a–c) The confocal microscope images of the coating H_{12}MDI/E (a), H_{12}MDI/E/1%N (b), and H_{12}MDI/E/3%N (c).

The values for surface roughness were calculated on the basis of confocal images. The obtained roughness parameters: R_a, R_z, R_t, R_q, R_{max}, R_{ms} S., and R_{pc} are higher in this case for sample H_{12}MDI/E/1%N and H_{12}MDI/E/3%N than those for the H_{12}MDI/E system (Table I).

Roughness

When analyzing the obtained results one may conclude that the lacquer surfaces are pretty smooth, since the R_a and R_z values are very low. Increasing in the roughness of the modified coatings were also observed (Fig. 7). Growth of the roughness is probably caused by presence of the particles of silicon in the coating surface (those particles have tendency to migration on the coating surface).[9] The roughness also increases with content of nano-fillers.

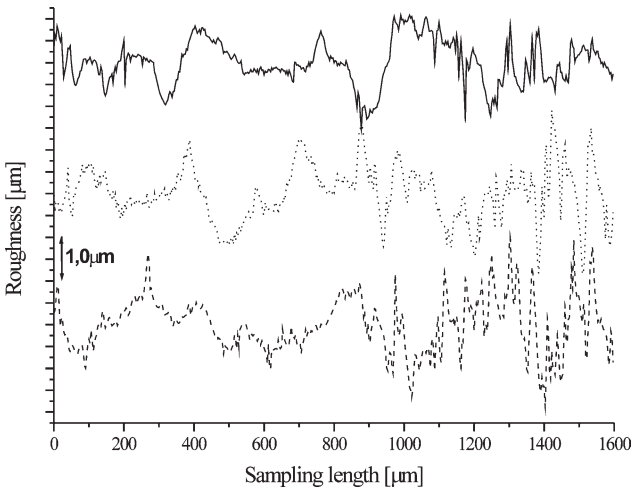

Figure 6 Comparison of the roughness profiles obtained on the basis of confocal images, H_{12}MDI/E, H_{12}MDI/E/1%N, H_{12}MDI/E/3%N.

Gloss

The samples of modified lacquers offer lower gloss values as measured at 20°, 65°, and 80° in relation to those for unmodified coats. The gloss parameter values decline for the growing shares of nano-powder (Fig. 8). Inferior gloss of the modified coats results from the increasing micro-inhomogeneity of the system due to the presence of siloxane structures along with polar polyurethane chains.[16]

Differential scanning calorimetry (DSC)

To be able to properly explain the transformations which take place, each sample was investigated in the heating–cooling–heating cycle. At the temperature of 54°C, the melting of the polyester resin Rucote 102 can be observed in DSC thermograms

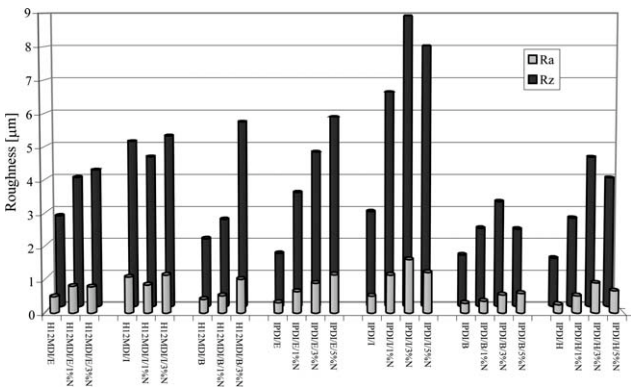

Figure 7 Comparison values of the coatings roughness.

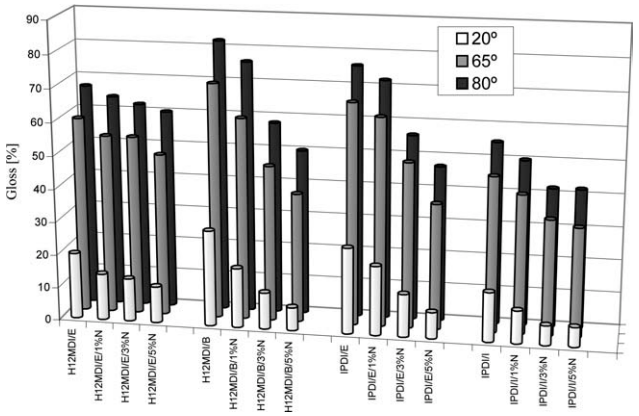

Figure 8 Comparison values of the coatings gloss.

(Fig. 9). There is no difference between crosslinking processes of modified and unmodified lacquers. The endothermic peak, which should occur at 110–150°C, was practically invisible due to the unblocking reaction. The curing reaction shows a small exothermic effect in the range of 150–200°C. Since deblocking was an endothermic process, and crosslinking was an exothermic one, the thermal effects of those reactions overlap. Hence, those two processes were not clearly visible. The peaks completely disappeared during the second heating—the coating was completely cured.

During the second heating cycle at the temperature range of 54–74°C, the glass transition of the polyurethane coating were observed. Comparing the T_g temperatures of modified with nanopowder polyurethanes (T_g = 62.3°C for H_{12}MDI/E/1%N, T_g = 65.6°C for H_{12}MDI/E/3%N, and T_g = 67.7°C for H_{12}MDI/E/5%N) with unmodified lacquer (T_g = 69.7°C for H_{12}MDI/E sample) it was observed that T_g were shifted toward lower temperatures. Incorporation of modificator probably caused decrease purity of amorphous phase composed of polyurethane. Shifting T_g toward higher values when the nanopowder content increase may be due to its migration to the coating surface and in consequence the purity of amorphous phase became higher.

No endothermic region of melting for the crystalline structures can be observed on DSC thermograms in spite of crystal structures were visible on optical micrographs, which were realized in the polarized light. It is caused by inconsiderable amount of crystalline phase.

Surface free energy

To find the values of surface free energy (SFE), wetting angles were measured for three model liquids: water, formamide, and diiodomethane. Water and formamide (bipolar liquids) form big drops on the coating surface (within 60.5° to 98.5°) (Table I), while much lower wetting angle values are specific for diiodomethane (nonpolar liquid), from 35.8° to 46.1°. As resulted from the data presented in Figure 10, the surface free energy values for the studied polyurethane coatings fall within the range of 31.92–41.55 mJ m^{-2}. Those values classify the studied coatings as medium-polarity ones. The obtained data suggest that a major contribution to the total surface energy is made by the "amount" of dispersion interactions, which is quantitatively expressed by the parameter γ_S^{LW}, and which is dependent on the structure of macromolecules. Acid–base interactions control the SFE value to a small degree only. The quantitative contribution from γ_S^{AB} never exceeds 0.5%.

The SFE values for the coatings which have not been modified differ from each other only slightly. Thus, no unequivocal conclusions may be drawn on the structural effects from crosslinking agents on SFE. Most probably, the decisive effect on the SFE

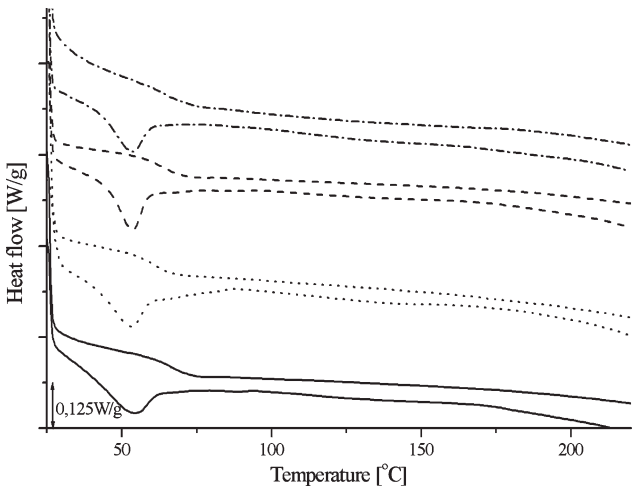

Figure 9 DSC thermograms of the coatings, H_{12}MDI/E, H_{12}MDI/E/1%N, H_{12}MDI/E/3%N, H_{12}MDI/E/5%N.

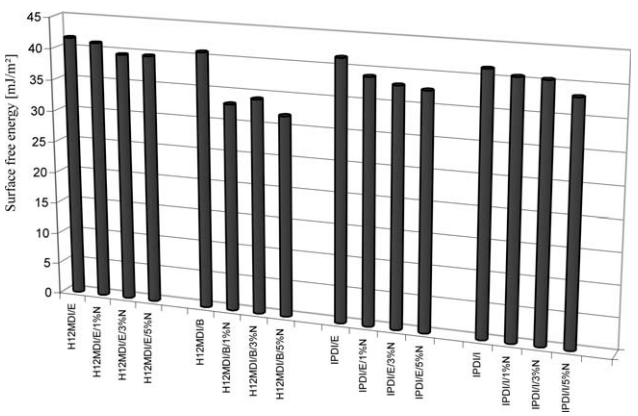

Figure 10 Comparison values of surface free energy for the studied coatings calculated from the measurements of wetting angles.

value comes from the polyester resin material which constitutes nearly 90% in all compositions.

The SFE value for the nano-particle containing coatings is slightly lower than that for the unmodified coatings. Decrease of SFE with nano-particle contents was observed. This fact is evidence of the water-repellent effects on the surfaces of the lacquer coatings, derived from nano-particles which contain the silicone resin.

CONCLUSIONS

Polyurethane powder coatings were modified by means of nano-particles with the cores of polysiloxane and shells of poly(methyl methacrylate), which were added to the lacquer formulations at the powder coating blending stage. The modern optical and confocal microscopy was employed to observe surface topography and supermolecular structures of the obtained lacquers Also, other instrumental techniques like, roughness analysis, gloss, and contact angles measurements were used in the determination of the surface properties. The confocal microscopy made the 3D visualization of the lacquer surfaces possible, and it enabled calculation of the surface roughness parameters. It should be noted that both the methods presented in this article are sufficiently general to be applicable in studying other polymer materials as well.

Reflection infrared spectra were confirmed to be present on the coatings surface bands from silicone resin. Based on DSC analysis it was found that synthesized coatings were generally amorphous. Increasing amount of nanopowder caused improving purity of amorphous phase, because of migration of silicone resin into the surface of the coatings.

Investigations confirmed that the surface of coatings made with modified lacquers have different structure than unmodified lacquers. The presence of silicon atoms in the lacquer coating structure was responsible for escalation of micro-inhomogeneity and roughness of the coat, and it reduces the size of supermolecular structures.

Modification of powder coatings, with polymer nano-powder, resulted in lower surface free energy values and lower gloss parameters, with simultaneously higher wetting angles, and roughness values of the obtained coats. Further increase of nanoparticles content may cause decreasing of surface free energy, growth micro-inhomogeneity and roughness, as well as fall of the gloss and haze appearance. The more homogeneous the coat was from the viewpoint of its chemical structure, the bigger its crystallites and the highest the surface quality and gloss were.

The optimal surface properties of polyurethane powder coatings were achieved for coatings containing 3 wt % of nanoparticles. The similar results were obtained by Kozakiewicz et al., during modification of epoxy powder coating with the same kind of nanoparticles.

The optical images were performed in the Biophysics Laboratory, Department of Physics, Rzeszow University of Technology. The laboratory has been equipped in the frame of the EU-Polish Integrated Regional Operational Programme (PIROP). The author thanks Mr. Ireneusz Niemiec, from NanoFocus, Oberhausen Germany, for carrying out confocal micrographs, Ms. Dorota Naróg, Ph.D., from the Faculty of Chemistry, Rzeszów University of Technology, for taking ATR FTIR spectra, as well as Bayer A.G., Evonik Degussa G.m.b.H., and Worlée-Chemie G.m.b.H for sending free samples of raw materials.

References

1. Fernando, R. H.; Sung, L.-P. Nanotechnology in Coatings; ACS: Washington, 2009.
2. Chemin, N. C.; Cassaignon, S.; Bourhis, E.; Jolivet, J.-P.; Spalla, O.; Barthel, E.; Sanchez, C. Chem Mater 2008, 20, 4602.
3. Martins, M. A.; Fateixa, S.; Giräo, A. V.; Pereira, S. S.; Trindade, T. Langmuir 2010, 26, 11407.
4. Fogelström, L.; Malmström, E.; Johansson, M.; Hult, A. ACS Appl Mater Interfaces 2010, 2, 1679.
5. Barna, E.; Bommer, B.; Kürsteiner, J.; Vital, A.; Trzebiatowski, O.; Koch, W.; Schmid, B.; Graule, T. Compos A Appl Sci Manuf 2005, 36, 473.
6. Sudeep, P. K.; Emrick, T. ACS Nano 2009, 3, 2870.
7. Kuczyñska, H.; Kozakiewicz, J. Ochrona przed Korozją 2008, 12, 440.
8. Li, Y.-Q.; Fu, S.-Y.; Yang, Y.; Mai, Y.-W. Chem Mater 2008, 20, 2637.
9. Kozakiewicz, J.; Kuczyñska, H.; Jesionowski, T.; Nowakowski, R.; Sobczak, J. W.; Koncka-Foland, A. Inżynieria Materiałowa 2007, 6, 863.
10. Pilch-Pitera, B. J Appl Polym Sci 2010, 116, 3613.
11. Pilch-Pitera, B. Przem Chem 2009, 8, 892.
12. Polish Committee for Standarization—Geometrical Product Specification (GPS)—Surface Texture: Profile Method—Motif Parameters, PN-EN ISO 12085, Warsaw, 2009, Poland.
13. Polish Committee for Standardization, Paints and Varnishes—Determination of Specular Gloss of Non-Metallic Paint Films at 20°, 60° and 85°, PN-EN ISO 2813, Warsaw, 2001, Poland.
14. Żenkiewicz, M. Adhezja i modyfikowanie warstwy wierzchniej tworzyw wielkocząsteczkowych, WNT, Warsaw 2000, Poland.
15. Król, P.; Pilch-Pitera, B. J Appl Polym Sci 2007, 104, 1464.
16. Pilch-Pitera, B.; Stagraczyñski, R. J Appl Polym Sci 2010, 118, 3586.